The current issue and full text archive of this journal is available at
www.emeraldinsight.com/0961-5539.htm

Temperature in a disk brake, simulation and experimental verification

Leszek Wawrzonek and Ryszard A. Białecki
Institute of Thermal Technology, Silesian University of Technology, Gliwice, Poland

Received 5 December 2006
Revised 25 May 2007
Accepted 25 May 2007

Abstract

Purpose – This paper seeks to develop a reliable simulation technique and experimental equipment applicable to thermal analysis of disk brakes. The application is focused on safety issues arising in coal mines and other hazardous explosive environments.

Design/methodology/approach – The experimental rig provides data on the friction power generated by the disk-pad pair for a user-defined squeezing force program. The developed software predicts the temperature field in the brake and pad. The code is based on the finite volume approach and is formulated in Lagrangian coordinates frame.

Findings – In the circumferential direction advection due to the rotation of the disk dominates over the conduction. The energy transfer problem could be formulated in a Lagrange coordinates system as 2D. A novel approach to the estimation of the uncertainty of numerical simulations has been proposed. The technique is based on the *GUM* methodology and uses sensitivity coefficients determined numerically. Very good agreement of simulated and measured values of temperature in the brake has been found.

Research limitations/implications – The results apply for simple disk and pad geometries for which the correlations of the Nusselt number versus Reynolds and Prandtl are known. Moreover, the model should not be used in the last braking period where the assumption of negligible circumferential conduction is not applicable. Though the code models a situation of constant rotation speed, the deceleration profile of the disk can readily be accounted for. The next step of the research should be to couple the heat conduction in the brake with CFD simulation of the surrounding air.

Practical implications – The highest temperature in the system is at the pad-disk interface. The depth of penetration of the temperature into the disk is relatively low. The heat dissipation from the disk is controlled by convection.

Originality/value – The novelty of the paper is in the simplified and robust simulation model of the brake, the concept of the experimental rig and the methodology of uncertainty assessment. The developed methodology can be useful to researchers and industry involved in safety investigations and determining safety standards, specifically in explosive atmospheres. It may also be of interest to the automotive industry.

Keywords Simulation, Thermal measurement, Finite volume methods

Paper type Research paper

1. Introduction

Heat transfer in brakes influences strongly their efficiency. The friction coefficient of the brake lining drops off quickly with temperature, reducing the braking efficiency. Moreover, the heat generated in brakes may lead to brake fluid vaporization or vapor lock, ending up with loss of braking action. The literature of the subject is vast. The interest is both in developing simplified models (Chichinadze, 1995; Naji and Al-Nimr, 2001;

International Journal of Numerical Methods for Heat & Fluid Flow
Vol. 18 No. 3/4, 2008
pp. 387-400

0961-5539
DOI 10.1108/09615530810853646

Matysiak *et al.*, 2002) and full CFD-based models (Abdel-Aal and Smith, 1998; Dittrich and Lang, 1984; Hopf and Gauch, 2000).

The motivation of this study did not come from the automobile application, but from coal mining. In an underground mine, the buildup of methane can, in a presence of a hot spot, trigger an explosion. Many mechanical devices used in coal mining are equipped with disk brakes. Predicting their maximum temperature, testing the quality of brake pad lining in the context to the temperature is of vital importance in every coal mine.

The aim of the paper is to develop a model of a disk brake of simplified geometry, validate it against an experiment and carry out sensitivity study. The purpose of the latter is to check how the changes of selected parameters (i.e. due to their uncertainty) influence the changes of the maximum temperature in the system.

2. Formulation

The geometry of the system is shown in Figure 1 left. The thickness of the rotor is $2H$. The brake rotor R is squeezed by a pair of brake pads P. Owing to symmetry, the computational region consists only of a half of the hollow brake rotor of thickness H and one brake pad.

Transient temperature field and constant material properties were assumed. The discussion in this paper is limited to a situation where the rotation speed was constant. The reason for this is that simulation results have been compared with experimental results. It was much easier to carry out the experiments keeping the rotation speed constant.

Using the Eulerian coordinates frame, the temperature field in the rotor satisfies the equation:

$$c_R\rho_R\frac{DT_R}{D\tau}=k_R\left[\frac{\partial^2 T_R}{\partial r^2}+\frac{1}{r}\,\frac{\partial T_R}{\partial r}+\frac{1}{r^2}\,\frac{\partial^2 T_R}{\partial \varphi^2}+\frac{\partial^2 T_R}{\partial z^2}\right];\quad r_i<r<r_o, 0<z<H, 0<\varphi<2\pi \tag{1}$$

where T_R, temperature within the rotor, k_R, heat conductivity, $c_R\rho_R$, specific heat and density, τ, time, r, radial coordinate, φ, angular coordinate, z, coordinate parallel to the axis of the rotor. Differential operator D stands for the material derivative.

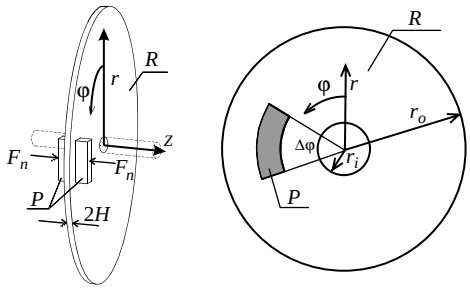

Figure 1.
Geometry of the disk brake

Notes: Left – original, right simplified. R – brake rotor; P – brake pad, F_n normal force squeezing the pads against the rotor

In order to simplify the generation of the numerical mesh, the geometry of the pad has been slightly modified. Its shape has been changed to a sector of a ring of the same surface area as the original pad. The sector is limited by an angle $\Delta\varphi$ (Figure 1 right).

As it will be shown in the next section, the circumferential conductive heat flux in the disk may be neglected. As a result, the computational domain could be limited to a sector of the disk. At some time instants this sector is in contact with the brake pad, in which case, the domain comprises both the sector of the disk and the pad. Here, are the boundary conditions prescribed on the surfaces bounding the computational domain.

The boundary conditions on the surface of the rotor are the following (Figure 2):

- symmetry plane S_1 and planes S_{11} and S_{12} – insulation;
- inner cylindrical surface S_3 – known temperature. Typically, in this hole a massive metal shaft is inserted. At the beginning of the process, the shaft temperature is that of the environment. As the braking process is short, the temperature rise due to the released heat of friction practically does not reach the shaft. Thus, the temperature on the internal surface of the hole has been assumed constant and equal to the environment temperature T_e;
- outer cylindrical surface S_4 – prescribed heat convection and radiation;
- except at the portion S_5 where the rotor is in contact with the brake pad, the free surface of the rotor S_2 exchanges heat with the environment by convection and radiation; and
- contact surface S_5 with the pad – generation of heat by friction. It is modeled by a plane heat source of known generation rate. As opposed to most published models, the fraction of the heat that is absorbed by the pad is not prescribed. Rather than this, the amount of heat that goes to the rotor and the pad are results of the model. The details of this condition, hereafter referred to as the friction condition, will be explained later.

The temperature field T_p in the pad is also transient. It is however assumed that the angular heat flux is negligible. As will be shown later, such an assumption is consistent with the heat transfer model in the rotor. On the contact surface, S_5 the friction condition is assumed. The opposite surface S_6 of the pad is fixed in a massive brake calliper initially at the temperature of the environment. Owing to the short time of braking, the temperature of this surface is assumed to be that of the environment. The remaining surfaces of the brake pad (S_7-S_{10}) exchange heat with the environment by radiation and convection. Implementation of this condition at surfaces,

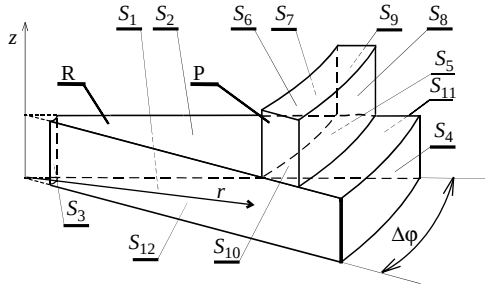

Figure 2.
Notation of boundary of surfaces used in the definition of the boundary conditions

S_9 and S_{10} require special treatment. As the gradients with respect to the angular coordinate, φ are neglected, these surfaces are by definition insulated. To allow for the heat exchange from this surfaces, the governing equation should be modified. The technique of deriving such an equation is analogous to the classic fin theory (Özişik, 1993). The brake pad is fixed in space thus, the material derivative does not enter the formulation:

$$c_P \rho_P \frac{\partial T_P}{\partial \tau} = k_P \left[\frac{\partial^2 T_P}{\partial r^2} + \frac{1}{r} \left(\frac{\partial T_P}{\partial r} - \frac{(T_P - T_e)(h_9 + h_{10})}{k_P \Delta \varphi} \right) + \frac{\partial^2 T_P}{\partial z^2} \right] \tag{2}$$

where h_9 and h_{10} denote the efficient heat transfer coefficient including both radiation and convection on surfaces S_9 and S_{10}, respectively.

The convective film coefficient is evaluated from equation (MSC NASTRAN THERMAL, MSC Software Corporation, available at: www.mscsoftware.com):

$$Nu_r = 0.0267 \ Re_r^{0.8} Pr^{0.6} \tag{3}$$

where $Nu_r = h_c r/k$, $Re_r = \rho \omega r^2/\eta$, $Pr = c\eta/k$, and h_c is the convective film coefficient, ω is the angular velocity and η stands for the dynamic viscosity.

The radiative component of the heat transfer coefficient is computed from a relationship:

$$h_{rad} = \sigma \varepsilon \frac{T^4 - T_e^4}{T - T_e} \tag{4}$$

where σ is the Stefan Boltzmann constant and ε stands for the emissivity. Two different values of emissivity have been used in the study: one corresponds to the trace made by the brake pad on the rotor, while the second describes the radiation of the remaining portion of the rotor. Owing to abrasion, the trace of the brake pad is shiny, meaning that the emissivity of the trace is lower than that of the remaining portion of the rotor.

The total heat transfer coefficient is thus described by an expression:

$$h_r = 0.0267 \ r^{0.6} \omega^{0.8} \rho^{0.8} \eta^{-0.2} c^{0.6} k^{0.4} + \sigma \varepsilon \frac{T^4 - T_e^4}{T - T_e} \tag{5}$$

which shows the dependence of the coefficient on both the radius and the local temperature.

The friction boundary condition prescribed on surface S_5 has been formulated as a plane heat source q_F releasing heat to both the rotor and the pad. The boundary condition at this surface is described by a jump in the normal heat flux and continuity of the temperature. This can be written as:

$$q_F - k_R \frac{\partial T_R}{\partial z} + k_P \frac{\partial T_P}{\partial z}; \quad T_R = T_P \ \text{valid on} \ S_5 \tag{6}$$

The heat rate generated due to friction is $q_F = p_n \mu r \omega$ with p_n denoting the pressure exerted by the brake pad on the surface of the rotor and μ standing for the friction coefficient.

The prescribed initial condition for both the rotor and the pad was homogeneous environment temperature T_e.

3. Numerical implementation

The main difficulty encountered when solving the problem was the presence of a moving and stationary part in the computational domain. None of commercial codes available at our institutions had an option to deal with such a situation. Thus, an *ad hoc* code based on the finite volume technique has been written (Wawrzonek, 2002). The problem at hand could be significantly simplified by changing the coordinates frame used to describe the heat transfer in the rotor. The idea was to use Lagragian (rotating coordinates) analysis instead of the Eulerian (stationary). This approach simplifies the numerical implementation, as the material derivative does not enter the formulation. As a result, the enthalpy fluxes do not arise in the energy balance of a rotor cell. The geometry of the segment is shown in Figure 2 right.

In the Lagrangian coordinates frame, the energy conservation equation in a segment of the rotor takes the form:

$$c_R \rho_R \frac{\partial T_R}{\partial \tau} = k_R \left[\frac{\partial^2 T_R}{\partial r'^2} + \frac{1}{r'} \frac{\partial T_R}{\partial r'} + \frac{\partial^2 T_R}{\partial z^2} \right] \tag{7}$$

where r' is the radial coordinate in the rotating coordinate frame.

One revolution of the disk is divided in two phases. In the first phase, a segment of the disk shown in Figure 2 accumulates a portion of the heat of friction. This phase lasts $\Delta\tau_h = \tau_t \Delta\varphi / 2\pi$ seconds. Where $\Delta\tau_h$ and τ_t denote the time of the heating phase and the time of one revolution of the disk, respectively. In the cooling phase, the segment is no longer in contact with the pad and dissipates heat to the environment. This phase lasts $\Delta\tau_c = \tau_t - \Delta\tau_h$ seconds.

It should be noted that though in the Lagrangian coordinate frame the angular dependence of the temperature field is neglected, it is not the case in the Eulerian system. In the stationary coordinates frame, the temperature field depends on the angular coordinate.

The remaining features of the implemented spatial and time discretization were standard, and as such will not be described here in detail (Özişik, 1993). It is enough to state here that backwards time differences and successive over relaxation with Gauss Seidel iteration were used. The over relaxation parameter for the the heating phase was 1.23, for the cooling phase 1.55. Both values were obtained experimentally. It should be noted, that the Newton Raphson solver implemented as an alternative to the Gauss Seidel scheme, lead to significantly longer running times.

Structured numerical mesh was used. The density of the mesh has been found experimentally in test calculations (Wawrzonek, 2002). The thickness H of the rotor (measured along the z-direction) was divided into 12 layers while the height of the pad into nine layers. The radial direction of the rotor was divided into 27 layers. In both cases, the higher density of the grid was applied in the areas of large temperature gradients. The thickest layer in z-direction was 1.5 mm while the thinnest 0.1 mm. The radial step of the mesh was between 30 and 1 mm. In the case of the temporal discretization, both the heating and the cooling phase were subdivided into five-time steps.

Obviously, the code can deal with any set of dimensions of the rotor and brake pad. For the purpose of comparison of the simulation and the experiments, the outer radius of the rotor was taken as $r_0 = 165$ mm while thickness of the rotor was $H = 10$ mm. The optimization of the numerical mesh is valid only for these dimensions.

Figure 3 shows the results of the calculations. Note that for the purpose of realistic visualization, the angular subdivision shown in the figures is three times denser than the actual computation mesh while the subdivision in the z- and r-directions is coarser than the optimal mesh.

The Figure shows that the rapid increase of temperature is limited only to a very thin rotor zone in contact with the pad.

3.1 Neglecting the circumferential conductive flux. Error assessment

In the developed heat transfer model, the conductive angular heat flux $q_a = -k(1/r)(\partial T_R/\partial \varphi)$ within one rotating segment was neglected. The influence of this simplification onto the resulting temperature field can be assessed using the temperature field for negligible angular heat conduction. When doing this one should keep in mind that in terms of the maximum temperature of the system, neglecting the circumferential flux is a conservative assumption. The temperatures in the vicinity of the hottest point (below the braking pad) obtained using the simplification, will be higher than in reality. The reason for this is that the conductive heat losses to the neighbouring segments are neglected.

Once the temperature field evaluated from the model with negligible circumferential conduction are known, the committed error resulting from the simplification can readily be assessed. The idea is to estimate the approximated angular heat fluxes between neighbouring segments by finite differences. Then, the already determined heat losses are substituted into the heat balance of the crucial (hottest) control volume. As a result, the temperature in this volume will be lower than in the the original model.

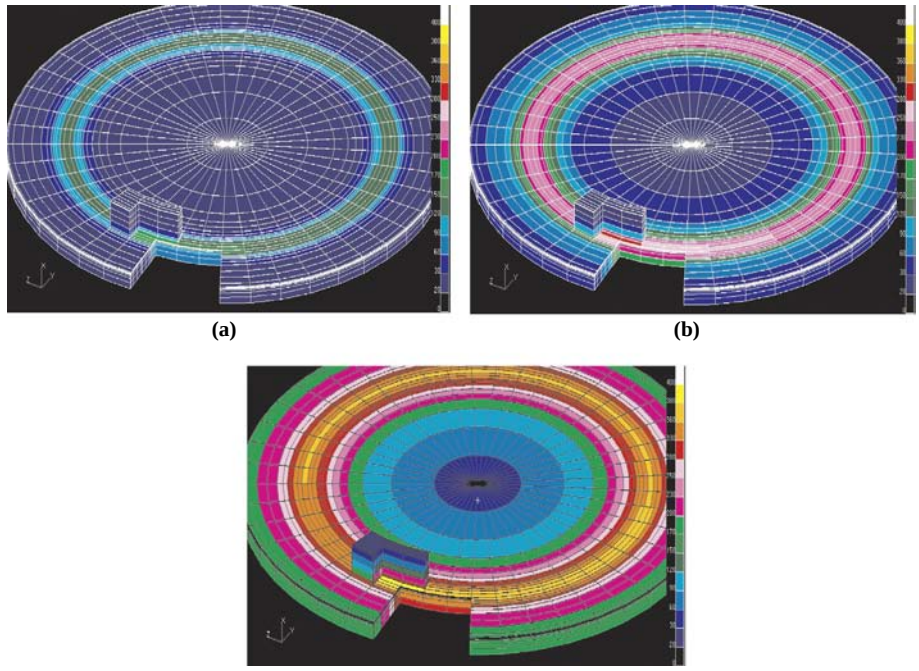

Figure 3.
Temperature field in the brake after: (a) 5 s; (b) 30 s and (c) 100 s

For the data used in the experiments (friction heat 10 MW/m^2 and linear velocity of the rotor at the center of the pad 10 m/s), the highest temperature in the system (the layer in contact with the braking pad), turned out to drop by 0.01 K. The reason for this can be best explained thinking about the Eulerian coordinates frame. In the motionless frame, the energy flux carried by the enthalpy is several orders of magnitudes higher than the conductive heat flux.

This statement holds true also for low velocities of the rotor, a situation characteristic to the end of braking. In this case, the friction heat is lower, as this quantity is proportional to the angular velocity. Taking pressure as 3 MPa the additional temperature drop would be of the order of 0.07 K for the velocity 1 m/s and 0.2 K for 0.1 m/s.

It is clear from the above analysis, that neglecting the angular conduction does not influence the accuracy of the model.

3.2 Sensitivity analysis

All data used to describe the model are known with a certain accuracy. It is important to know, how the error in the input data influences the final results, specifically the highest temperature at a given time instant.

The problem can be addressed using the sensitivity analysis. The fundamental notion of this approach is the evaluation of the sensitivity coefficients. They are defined as $\alpha_i = (\partial y/\partial x_i)$, where y is the response variable and x_i is the i-th independent variable y depends on. The parameters under consideration were:

- instantaneous friction power N_f;
- heat conductivities k of rotor (R) and brake pad (P);
- specific heat c of rotor (R) and brake pad (P);
- emissivity of the rotor surface within the trace of the pad ε_t and outside it ε_o;
- multiplier of the heat transfer coefficient β; and
- angular velocity ω.

From this list of considered variables, only the multiplier β requires additional explanation. In fact, it is the heat transfer coefficient h_R on the rotor, that should be taken as an independent variable. However, heat transfer coefficient on the rotating disk is itself a function of the radius (equation (5)). Sensitivity coefficient can only be evaluated with respect to a scalar variable. Thus, the function should be parameterized, i.e. expressed as a combination of unknown parameters and known functions and the sensitivities determined taking these unknown coefficients as independent variables. In the case of heat transfer coefficient, the simplest possible parametrization of the distribution of the heat transfer coefficient has been applied. The idea is to express the variation of the coefficient as a product of an unknown scalar β and the original function (equation (5)).

Maximum temperature T_{max} appearing in the system at a given time instant has a decisive effect on the safety of the brake operation in the mine. Thus, this parameters has been chosen as the response variable in the sensitivity analysis. The location of the node where such a temperature appears was not defined a priori but determined by appropriate search over all nodal points.

The sensitivity coefficients with respect to a given variable x_i have been approximated using finite differences as:

$$\alpha_i = \frac{T^{u}_{max} - T^{l}_{max}}{x^{u}_i - x^{l}_i} \tag{8}$$

where x^{u}_i, x^{l}_i upper and lower limits of the variable, T^{u}_{max}, T^{l}_{max} values of the maximum temperature calculated using x^{u}_i, x^{l}_i, respectively. When evaluating the sensitivity coefficients, the values of other parameters ($x_j, j \neq i$) took the average values within their variation range $x_j = (x^{u}_j + x^{l}_j)/2$.

Table I shows the values of the lower and upper limits of the variables under consideration.

The sensitivity coefficients depend strongly on time. With constant braking force and friction coefficient, the work of friction is proportional to time. However, as the friction coefficient depends strongly on temperature, taking time as an independent variable would lead to misleading conclusions. Therefore, the variation of the sensitivity coefficients in the course of the experiment has been shown as a function of the work of friction. Figure 4 shows the plots of the sensitivity coefficient versus the dissipated work of friction.

4. Experiment

A pulley transmission couples the rotational power of an electric motor to the brake disk. The kinematic scheme of the device to measure the normal force F_n and the friction force F_f is shown in Figure 5. The brake pad (P) is pressed against the rotor (R) by a pneumatic servo (S). The normal force is measured by sensor (M_p) directly. The friction force is transmitted to the sensor (M_f) by lever (L). The value of the force is evaluated from moment equilibrium. The temporal variation of this value was then used in the simulation define the value of the heat generated at the contact surface of the rotor and the pad.

The temperature was measured by a pyrometer pointing at the braking trace. The device has the range 0-800°C, the spectral measuring range was 8-14 μm accuracy 1 percent of the reading, time constant 367 ms and the diameter of the measuring area 6.4 mm at the distance 200 mm. The sensor has been calibrated using material of known emissivity.

The pyrometer was pointed to the hottest visible point, ie., the location on the rotor immediately after the pad. The axis of the sensor was slightly inclined with respect to the axis of the rotor. As a result, the area the sensor collected the signal from, was an ellipse of dimensions 11.9 by 10.4 mm. As this corresponds to several numerical cells, the measured and calculated temperatures could not be compared directly. To make a fair comparison, the measured temperature was compared against the value of a weighted mean value of the calculated temperatures. The weighting factors were the surface areas of appropriate numerical cells falling into the mentioned above ellipse.

All measured values were recorded using a multichannel data acquisition system connected to a PC.

Table I. Limits of variation of parameters used in the sensitivity analysis

Variable	N_f	k_R	k_P	c_R	c_P	ε_t	ε_o	β	ω
Unit	W	W/mK	W/mK	J/kg K	J/kg K	–	–	–	l/s
Lower limit	1,000	14	0	450	500	0.08	0.1	0.606	83.3
Upper limit	8,000	18	2	650	1,300	0.32	0.4	0.848	333.3

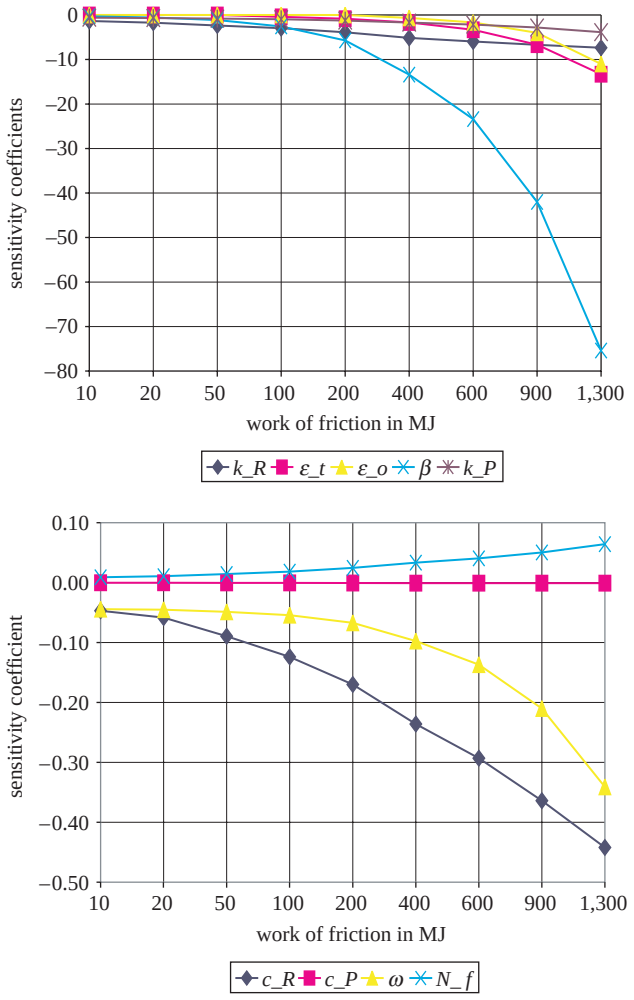

Notes: The curved are marked by the symbol of the independent variables: *k_R* heat conductivity of the rotor, *ε_t* emissivity with in the brake pad trace, *ε*_0 emissivity outside the trace, *β* with parameter of the heat transfer coefficient, *k_P* conductivity of the pad, *c_R* specific heat of the rotor, *c_P* specific heat of the pad, *ω* angular velocity, *N_f* instantenus power of friction

Figure 4.
Sensitivity coefficients of several parameters versus the generated heat of friction

The values of the emissivities were obtained in a separate test. After the main experiment has been finished, thin black paint film was applied at eight symmetrical locations on the braking trace. The pyrometer was then pointed to the foil and a location next to it. Assuming that the temperature at these two locations was the same, the emissivity of the trace could be retrieved. It was observed, that the values, especially within the braking trace, changed significantly in time. Other material properties were taken from the manufacturer data.

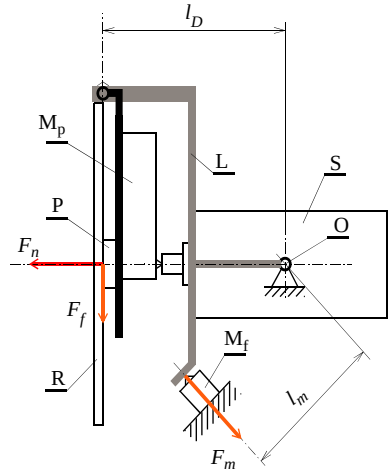

Figure 5.
Scheme of the experimental rig

5. Error analysis

The uncertainty analysis has been carried out for both the measurements and the simulations. The employed procedure is referred to at (*GUM*, 1995) as the Type B evaluation of standard uncertainty. The technique known as the *GUM* method is widely accepted and recommended by international organizations as ISO, NIST, IUPAC and many others, but so far it has been used only to assess the experimental errors. The paper proposes to use of this methodology to estimate the values of numerical models. The technique is based on the law of propagation of uncertainty stating that the uncertainty is defined as the positive root of the estimated variance u_c obtained from:

$$u_C^2(y) = \sum_{i=1}^{N} \left(\frac{\partial f}{\partial x_i}\right)^2 u^2(x_i) + 2\sum_{i=1}^{N-1}\sum_{j=i+1}^{N} \frac{\partial f}{\partial x_i}\,\frac{\partial f}{\partial x_j}\,u(x_i, x_j) \tag{9}$$

where x_i is the estimate of the input value, $u(x_i)$ is its standard variance, y is the estimate of the output quantity, $u(x_i,x_j)$ is the estimated covariance of variables x_i and x_j. The partial derivatives of the functional relationship between the input and output values, known also as the sensitivity coefficients, are to be evaluated at x_i.

The measure of the uncertainty, termed as the expanded uncertainty is obtained by multiplying the standard uncertainly u_c by the so-called coverage factor k. This quantity is evaluated by estimating the efficient value of degrees of freedom and using the t-distribution for the required level of confidence (95 percent was used in this study).

The result of the procedure is the uncertainty interval of the simulated data. Analogous uncertainty of the measured maximum temperature has been obtained using standard procedures.

The working equation for determining the uncertainty intervals used in the paper takes the form:

$$u_C^2(T_{max}) = \sum_{i=1}^{N} \alpha_i^2 u^2(x_i) + 2\sum_{i=1}^{N-1} \sum_{j=i+1}^{N} \alpha_i \alpha_j u(x_i, x_j) \quad (10)$$

where the components x_i are all parameters considered in the sensitivity analysis (N_t,k_R,k_P, etc.). The values of the sensitivity coefficients arising in equation (9) have been taken from the numerical simulations described in the previous section. Variations and covariations have been determined analyzing the probability distribution of the variables. The obtained values of the uncertainty intervals have been utilized in the visualization of the results of experiments and simulations as shown in the next section.

6. Results

Several experiments have been carried out and compared against the simulated values. The first experiment was carried out for angular velocity $\omega = 174\,\mathrm{s}^{-1}$ corresponding to linear velocity of 20.9 m/s. The applied normal force was 454 N the mean friction power was 3.3 kW. The resulting temperature at the braking trace is shown in Figure 6. The material of the rotor was a low alloy higher strength carbon steel 18G2A (notation after Polish Standard PN-82/H-84017).

In Experiment 2, larger normal force 1,374 N was applied. The initial friction power about 10 kW. Owing to the high temperature, the friction coefficient dropped in the course of the experiment. As a result, the friction heat rate also decreased. The mean friction power was at 4.3 kW. The results are shown in Figure 7.

In both experiments, the pressure was stabilized, so that its value did not change more than few percent. Experiment 3 was designed to check the ability of the model to reproduce the dynamics of the temperature field. In this test run, the values of the normal force was varied between 91 and 1,028 N. The comparison of the measured and simulated temperatures is shown in the upper right part of Figure 8.

The results of the simulation and experiments compared well in several other cases described in (Wawrzonek, 2002). In all these experiments, the material of the rotor was

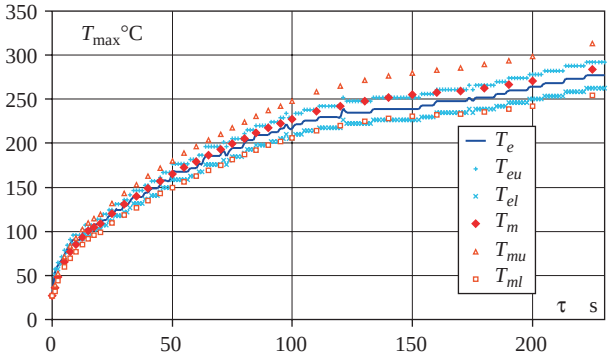

Notes: Experiment 1. Notation: T_m, T_e, modeled (simulated) and experimental values, T_{ml}, T_{mu} upper and lower bounds of the uncertainty interval of the modeled values. T_{el}, T_{eu} upper and lower bounds of the uncertainty interval of the experimental values

Figure 6.
Temperature at the center of the braking trace

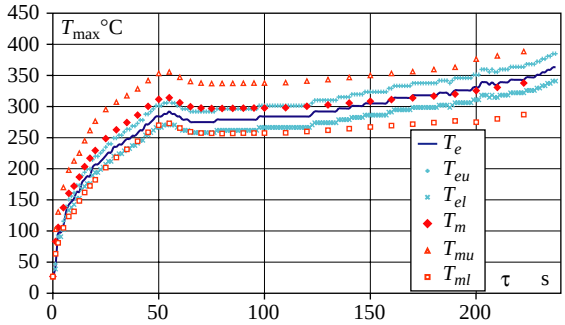

Figure 7.
Temperature at the center of the braking trace

Notes: Experiment 2. Notation: T_m, T_e, modeled (simulated) and experimental values, T_{ml}, T_{mu} upper and lower bounds of the uncertainty interval of the modeled values. T_{el}, T_{eu} upper and lower bounds of the uncertainty interval of the experimental values

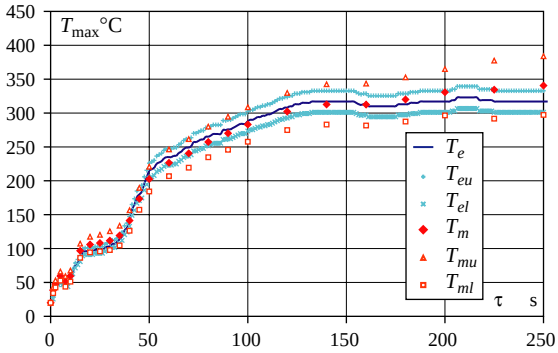

Figure 8.
Temperature at the center of the braking trace

Notes: Experiment 3. Notation: T_m, T_e, modeled (simulated) and experimental values, T_{ml}, T_{mu} upper and lower bounds of the uncertainty interval of the modeled values. T_{el}, T_{eu} upper and lower bounds of the uncertainty interval of the experimental values

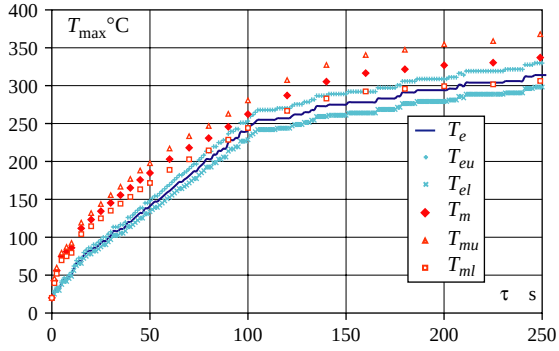

Figure 9.
Notation: T_m, T_e, modeled (simulated) and experimental values, T_{ml}, T_{mu} upper and lower bounds of the uncertainty interval of the modeled values

Notes: T_{el}, T_{eu} upper and lower bounds of the uncertainty interval of the experimental values

the same mild steel. The accuracy of the model deteriorated when the rotor was made up of a austenitic steel (1H18N9T – notation after PN H 86020). The heat conductivity of this steel is about two times lower than that of 18G2A. The results of the comparison are shown in Figure 9. The possible explanation is, that in this case the emissivity of the material could changed significantly in the course of the experiment. Though the response of the model weakly depends on the emissivity, the temperature measured by the pyrometer is very sensitive to the value of the emissivity.

It should be stressed that from the practical point of view the case of low-conduction rotor is of no importance. To avoid overheating, the contemporary brake rotors are manufactured from highly conducting materials.

7. Conclusions

The developed model of the disk brake reproduced well the behavior of the physical model, specifically for carbon steel where the differences between the measured and simulated results were lower than 30 K. Austenitic steel requires additional experiments in order to determine the proper emissivity of the material.

Neglecting the angular heat conduction leads to significant simplification of the numerical model and execution times of the simulations. This assumption does not have practically any influence on the resulting temperature field, thus this procedure should be recommended.

The sensitivity analysis has shown that the crucial variable, the maximum instantaneous temperature of the brake, depends strongly on the value of the heat transfer coefficient.

Methodology of error analysis based on reference (*GUM*, 1995) has been applied to investigate the accuracy of numerical simulation. The technique originally designed to deal with experimental results, has shown the uncertainty bounds of the model. Simultaneous application of the same technique of error analysis to simulation and experiments yields the mutual interrelation of the uncertainty of both types of results.

Though the model has been elaborated to deal with constant rotation speed of the disk, a more realistic case of deceleration can also be treated by the developed code. To do this, the deceleration profile should be defined (it may come from the energy balance of the entire device). Once this is known, the rotation speed can be adjusted to that defined in the profile after, say, every full turn of the rotor.

References

Abdel-Aal, H.A. and Smith, S.T. (1998), "On friction-induced temperatures of rubbing metallic pairs with temperature-dependent thermal properties", *Wear*, Vol. 216 No. 1, pp. 41-59.

Chichinadze, A.A. (1995), "Process in heat dynamics of modelling of friction and wear (dry and boundary friction)", *Tribology International*, Vol. 28 No. 1, pp. 55-8.

Dittrich, H. and Lang, R. (1984), "Finite-Elemente-Berechnung der thermischen Belastung einer Personenwagen-Scheibenbremse", *ATZ Automobiltechnische Zeitschrift*, Vol. 86, pp. 120-30.

GUM (1995), *Guide to the Expression of Uncertainty in Measurement*, International Organization for Standarization, Geneva, ISBN 92-67-10188-9.

Hopf, A. and Gauch, A. (2000), *Numerische Simulation der Bremsenkuelung mit CFD und FEM*, VDI Verlag GmbH, Duesseldorf, VDI-Berichte 1559.

Matysiak, S.J., Yevtushenko, A.A. and Ivanyk, E. (2002), "Contact temperature wear of composite friction elements during braking", *International Journal of Heat and Mass Transfer*, Vol. 45, pp. 193-9.

Naji, M. and Al-Nimr, M. (2001), "Dynamic thermal behavior of a brake system", *International Communications in Heat and Mass Transfer*, Vol. 28 No. 6, pp. 835-945.

Özişik, N.M. (1993), *Heat Conduction*, 2nd ed., Wiley, New York, NY.

Wawrzonek, L. (2002), "Mathematical model of heat transfer in a disk brake as a prediction tool in explosion forecasting", PhD thesis, Main Mining Institute (Główny Instytut Górnictwa), Katowice (in Polish).

Corresponding author
Ryszard A. Białecki can be contacted at: bialecki@itc.polsl.pl